SHORT COMMUNICATION

Spontaneous Regression of a Verrucous Venous Malformation Associated with a Previously Undescribed *MAP3K3* Variant

Andrea DIOCIAIUTI[1], Emanuele BELLACCHIO[2], Claudia CESARIO[3], Sabrina ROSSI[4], Giovanna ZAMBRUNO[1] and May EL HACHEM[1]

[1]Dermatology Unit and Genodermatosis Research Unit, Translational Paediatrics and Clinical Genetics Research Division, Bambino Gesù Children's Hospital, IRCCS, Rome, [2]Molecular Genetics and Functional Genomics, Bambino Gesù Children's Hospital, IRCCS, Rome, [3]Laboratory of Medical Genetics, Translational Cytogenomics Research Unit, Bambino Gesù Children's Hospital, IRCCS, Rome, and [4]Pathology Unit, Bambino Gesù Children's Hospital, IRCCS, Rome, Italy. E-mail: andrea.diociaiuti@opbg.net

Submitted Jun 8, 2025. Accepted after revision Aug 26, 2025
Published Oct 6, 2025. DOI: 10.2340/actadv.v105.44095. Acta Derm Venereol 2025; 105: adv44095.

Verrucous venous malformation (VVM), formerly known as verrucous haemangioma, is a congenital sporadic vascular anomaly appearing as a well-circumscribed, hyperkeratotic, reddish-purple plaque mostly located on the lower extremities (1, 2). Hyperkeratosis increases over time, resulting in the typical verrucous appearance frequently associated with scaling and crusting. Histopathological examination shows a hyperkeratotic epidermis overlying dilated vessels extending from the superficial to the deep dermis and subcutaneous tissue. Immunohistochemistry usually shows focal GLUT1 positivity and variable reactivity for WT1 (3, 4).

Genetic studies have identified a recurrent pathogenetic missense variant, p.I441M, in the *MAP3K3* gene in VVM lesions (5). *MAP3K3* encodes for mitogen-activated kinase kinase kinase 3 that belongs to the RAS/MAPK/ERK signalling pathway, which regulates cell proliferation, differentiation, and survival.

We report the case of an infant affected with VVM associated with a previously unreported somatic *MAP3K3* inframe duplication and showing an exceptional spontaneous regression.

MATERIALS, METHODS AND RESULTS

Following the parents' informed consent, 2 x 3-mm punch biopsies were obtained from lesional skin for histopathological examination and genetic analysis at age 1 month, and an additional punch biopsy for genetic analysis was taken from atrophic skin at age 4 years. Genetic testing was performed on genomic DNA from skin and peripheral blood. Custom panel next-generation targeted resequencing on a NextSeq550 (Illumina, San Diego, CA, USA) sequencing platform was carried out as previously described (6).

To investigate possible effects of the c.13_54dup mutation in *MAP3K3* and to model this protein mutant, the structure of *MAP3K3* in complex with the cerebral cavernous malformations-2 (CCM2) protein (Protein Data Bank, PDB, accession code 4Y5O) was employed. The hydrophobic dipole moment (μ) for a-helices was calculated according to the formula $\mu = \sum i\ Hi\boldsymbol{S}i$ (7) where $\boldsymbol{S}i$ is a unit vector pointing from the alpha carbon atom of the i^{th} residue to the residue side chain centre. For the wild type *MAP3K3* protein, the calculation was made across the helix-forming residues 1–15 as available in the PDB structure 4Y5O, while for the *MAP3K3* mutant the calculation was made across the modelled helical residues 1–33.

A neonate born at term by vaginal delivery was referred to our Vascular Anomalies Center for a congenital vascular anomaly of the right leg. At 1 month of age, physical examination showed a violaceous plaque almost entirely covered by dark crusts and scales with geographic borders (**Fig. 1**A). The newborn was in good general health.

Histological examination of a lesional skin biopsy showed a hyperkeratotic and papillomatous epidermis overlying dilated vessels extending from the papillary dermis to the subcutaneous tissue (Fig. S1). The vascular component was positive for pan-endothelial markers CD31 and CD34 and focally for GLUT1, WT1 and D2–40 (Fig. S2). Histopathology findings were consistent with the clinical suspicion of VVM.

Genetic analysis detected the *MAP3K3* inframe variant c.13_54dup (p.Glu5_Gln18dup) in the lesional skin at a variant allele frequency (VAF) of 12% and not in blood DNA (Fig. S3). The duplication was not reported in the literature and not annotated in the database of human variations (GnomAD).

MAP3K3 protein binds cerebral cavernous malformations 2 (CCM2) harmonin homology domain (8) through the PB1 domain and the amino acid segment 6-ALNSIMNDL-14 comprised in the N-terminal α-helix (**Fig. 2**). Translation of the c.13_54dup mutant results in a protein product with amino acids 5–18 duplication, which implies an additional ALNSIMNDL amino acid segment. Protein secondary structure predictions indicate that the duplication causes the formation of a longer α-helix in the N-terminal region compared with the wild type. One of the conceivable effects of this mutation would be an alteration of the *MAP3K3*/CCM2 interaction. As the PB1 domain and the N-terminal helix are connected by a long flexible linker, it is possible that in the mutant any of the 2 ALNSIMNDL segments could find suitable position, in concert with PB1, to still interact with CCM2. Thus, despite the important structural alteration, the *MAP3K3* mutant might still be able to bind CCM2, although with different affinity compared with the wild type protein. Furthermore, the calculation of the hydrophobic dipole moment indicates that the mutated helix increases significantly its amphipathic characteristics (Fig. 2C).

Unexpectedly, the VVM underwent a spontaneous regression process, which was already visible at the age of 2 months. At first the hyperkeratosis disappeared together with central fading of the vascular component (Fig. 1B) that regressed almost completely by the age of 2 years (Fig. 1C). The child, who is now 4 years old, presents a hypopigmented sclero-atrophic skin with very few peripheral dilated capillaries (Fig. 1D). A biopsy of the atrophic skin has shown that the *MAP3K3* duplication is no longer detectable.

DISCUSSION

Our case has 2 major peculiarities: the disease course and the previously undescribed somatic *MAP3K3* variant. To the best of our knowledge, spontaneous regression of VVMs has never been reported. Since

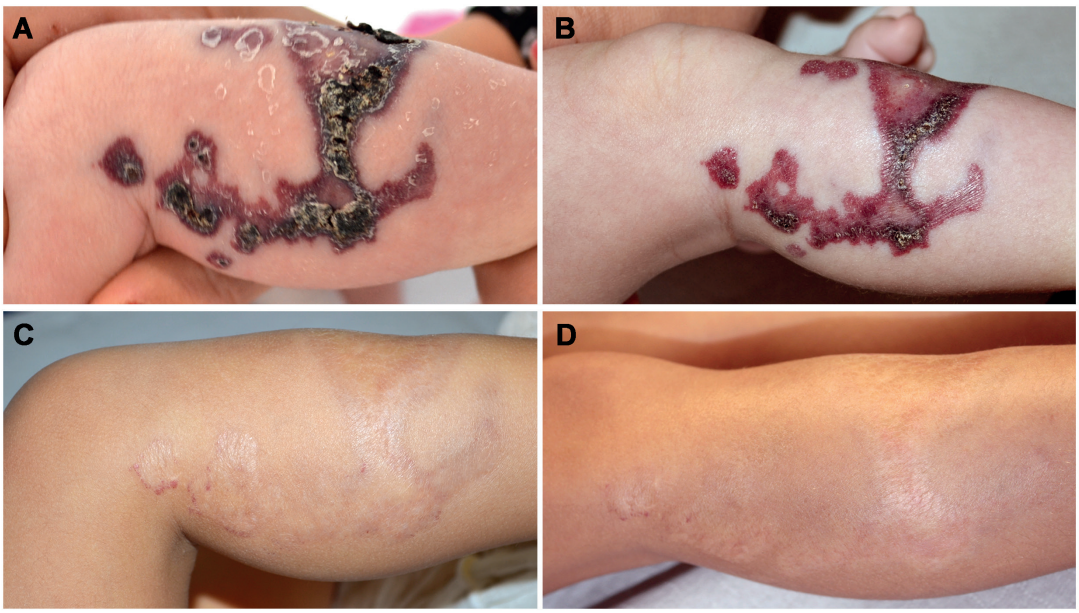

Fig. 1. Clinical features and course of verrucous venous malformation in the study patient. (A) Violaceous hyperkeratotic plaque with geographic margins and satellite lesions at age 1 month; (B) partial regression of hyperkeratosis and initial fading of the vascular component at the age of 2 months; (C) almost complete regression of the vascular anomaly with residual skin atrophy and dilated capillaries at the periphery at age 2 years, the latter being (D) further reduced at 4 years of age.

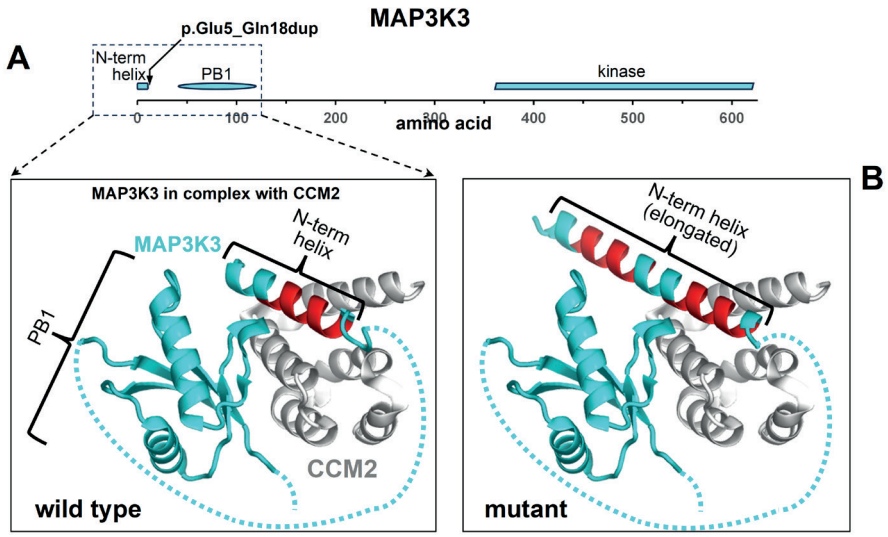

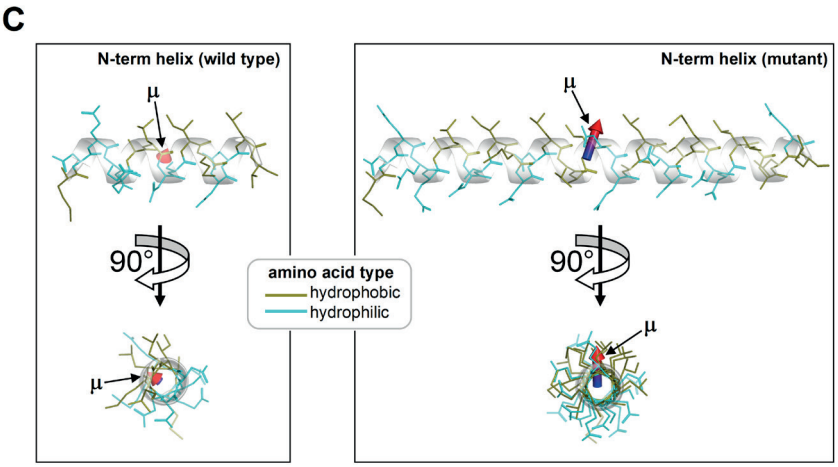

Fig. 2. Wild type and mutated MAP3K3 molecular modelling. (A) Schematic representation of MAP3K3 protein. (B) MAP3K3 in complex with the harmonin domain of the cerebral cavernous malformations 2 protein (CCM2) (from Protein Data Bank, PDB, accession code 4Y5O) and modelling of the same complex with MAP3K3 carrying the 5–18 duplication. The residues in the N-terminal helix that are strictly involved in the binding to CCM2 (6-ALNSIMNDL-14, as numbered in the wild type MAP3K3, and duplicated in the mutant) are coloured in red. The azure dotted lines represent MAP3K3 protein disordered regions. (C) Hydrophobic dipole moment (μ) calculated for the N-terminal helix in the wild type and mutated MAP3K3. It can be seen that the helix in the mutant presents increased μ, implying augmented amphiphilicity, which enhances the possibility of abnormal interactions with cell membranes or other lipidic particles.

the first days of life, the VVM presented a marked hyperkeratosis that rapidly reduced, while VVMs frequently become more hyperkeratotic over time (1, 2). Even more surprisingly, a concomitant clearing of the vascular component starting from the centre to the periphery was observed. Overall, the VVM almost entirely disappeared by the age of 2 years leaving a hypopigmented sclero-atrophic skin.

In addition, our child did not carry the *MAP3K3* recurrent missense mutation p.I441M, but a previously unreported somatic inframe duplication, c.13_54dup. CCM2, in complex with CCM1 and CCM3, inhibits *MAP3K3* (9) by the interaction between the *MAP3K3* N-terminus and the harmonin homology domain of CCM2 (8). Disruption of such interaction in endothelial cells of the developing mouse heart results in increased *MAP3K3* signalling (10). In keeping, a pathogenic variant in the CCM2 harmonin domain in a family with cerebral cavernous malformations has been shown to abrogate the CCM2/*MAP3K3* interaction, resulting in *MAP3K3* signalling activation and further supporting a crucial role of *MAP3K3* regulation in human disease (9). Based on literature data and on clinical and protein modelling findings, we propose that the pathogenic mechanism of the p.Glu5_Gln18dup variant in the *MAP3K3* N-terminus here reported arises from a decrease in *MAP3K3*/CCM2 interaction leading to reduced *MAP3K3* inhibition, resulting in VVM formation during intrauterine life.

The remarkably spontaneous and rapid VVM regression after birth suggests that different conditions between intrauterine and postnatal life should be responsible for the unexpected clinical course. We hypothesize that the CCM complex exerts the strongest physiological negative regulation on *MAP3K3* during prenatal development when vasculogenesis and angiogenesis are particularly intense. After birth, a naturally decreased CCM complex expression/activity may result in a further increase of the mutant *MAP3K3* activity. We suggest that, after birth, the mutant cells subjected to unsustainable *MAP3K3* activity undergo apoptosis. This hypothesis is supported by the observation that the *MAP3K3* I441M variant promotes endothelial apoptosis in mice (11). Alternatively, it may be speculated that negative clonal selection of mutant MAP3K3 cells occurs after birth, favouring skin repopulation by non-mutated cells. In keeping with these hypotheses, the *MAP3K3* duplication variant was no longer detectable in the atrophic skin at the end of the regression process.

In conclusion, we report for the first time an inframe duplication in *MAP3K3* associated with a unique behaviour of the VVM. Further studies will allow to understand the frequency of this association and the underlying pathogenetic mechanisms.

ACKNOWLEDGEMENT

The authors would like to thank the patient's parents for giving informed consent for clinical picture publication and Mr Gabriele Bacile for artwork.

Funding sources: This work was supported in part by the Italian Ministry of Health with "5 per mille" funds code "5M-2019-23680199" to May El Hachem and also by the Italian Ministry of Health with "Current Research funds".

IRB approval status: Permission to publish pictures was obtained from the patient's parents.

The authors have no conflicts of interest to declare.

REFERENCES

1. Imperial R, Helwig EB. Verrucous hemangioma: a clinicopathologic study of 21 cases. Arch Dermatol 1967; 96: 247–253. https://doi.org/10.1001/archderm.1967.01610030025004
2. Tennant LB, Mulliken JB, Perez-Atayde AR, Kozakewich HP. Verrucous hemangioma revisited. Pediatr Dermatol 2006; 23: 208–215. https://doi.org/10.1111/j.1525-1470.2006.00219.x
3. Colmenero I, Knöpfel N. Venous malformations in childhood: clinical, histopathological and genetics update. Dermatopathology (Basel) 2021; 8: 477–493. https://doi.org/10.3390/dermatopathology8040050
4. Wang L, Gao T, Wang G. Verrucous hemangioma: a clinicopathological and immunohistochemical analysis of 74 cases. J Cutan Pathol 2014; 41: 823–830. https://doi.org/10.1111/cup.12385
5. Couto JA, Vivero MP, Kozakewich HP, Taghinia AH, Mulliken JB, Warman ML, et al. A somatic MAP3K3 mutation is associated with verrucous venous malformation. Am J Hum Genet 2015; 96: 480–486. https://doi.org/10.1016/j.ajhg.2015.01.007
6. Diociaiuti A, Rotunno R, Pisaneschi E, Cesario C, Carnevale C, Condorelli AG, et al. Clinical and molecular spectrum of sporadic vascular malformations: a single-center study. Biomedicines 2022; 10: 1460. https://doi.org/10.3390/biomedicines10061460
7. Eisenberg D, Weiss RM, Terwilliger TC, Wilcox W. Hydrophobic moments and protein structure. Faraday Symp Chem Soc 1982; 17: 109–120. https://doi.org/10.1039/fs9821700109
8. Fisher OS, Deng H, Liu D, Zhang Y, Wei R, Deng Y, et al. Structure and vascular function of MEKK3-cerebral cavernous malformations 2 complex. Nat Commun 2015; 6: 7937. https://doi.org/10.1038/ncomms8937
9. Zhou Z, Tang AT, Wong WY, Bamezai S, Goddard LM, Shenkar R, et al. Cerebral cavernous malformations arise from endothelial gain of MEKK3-KLF2/4 signalling. Nature 2016; 532: 122–126. https://doi.org/10.1038/nature17178
10. Zhou Z, Rawnsley DR, Goddard LM, Pan W, Cao XJ, Jakus Z, et al. The cerebral cavernous malformation pathway controls cardiac development via regulation of endocardial MEKK3 signaling and KLF expression. Dev Cell 2015; 32: 168–180. https://doi.org/10.1016/j.devcel.2014.12.009
11. Xu H, Yang Y, Zhou Q, Huo R, Zhao S, Sun Y, et al. Map3k3 I441M knock-in mouse model of cerebral cavernous malformations. Stroke 2025; 56: 1010–1025. https://doi.org/10.1161/STROKEAHA.124.049935